RSC Advances

ROYAL SOCIETY OF CHEMISTRY

www.rsc.org/advances

Journal Name

ARTICLE

Three-dimensional carbon boron nitride with the broken hollow spherical shell for water treatment

Received 00th January 20xx,
Accepted 00th January 20xx

DOI: 10.1039/x0xx00000x

www.rsc.org/

Huichao Jia[a], Jie Li[a], Zhenya Liu*[a], Ruoyuan Gao[a], Saleem Abbas[a], Yi Fang[a], Chao Yu[a], and Chengchun Tang*[a]

Three-dimensional carbon boron nitride (3D C-BN) with the unique morphology were fabricated by a simple method, which are composed of the broken hollow spherical shells. The 3D C-BN possesses abundant surface adsorption sites, exhibiting very excellent adsorption rates of the methylene blue (MB) in aqueous solution. The most extreme advantages are that the absorption rate of the MB becomes faster when it was used by the second time. Moreover, the excellent reusability of the 3D C-BN confirmed that it can be reused eight times at least, and the adsorption capacity still preserves a high level up to 95%. Our finding indicates that the 3D C-BN is a promising adsorption material for water purification.

1. Introduction

Low-dimensional nanomaterials such as zero-dimensional (0D) particles, one-dimensional (1D) fibres, wires or tubes, and two-dimensional (2D) membranes or nanosheets, have been widely applied to construct nanodevices and functional nanomaterials.[1-3] Nowadays, three-dimensional (3D) nanostructured materials, including 3D metal/hydroxide,[4] 3D polymer[5] and 3D ceramics,[6] have received very much attention due to their interesting properties and advanced potential applications.[7,8] For example, 3D carbon as a practical 3D nanostructured material, has been extensively applied in adsorption, catalysis, energy and biomedical fields.[9,10] Especially, because of the urgent needs to solve daily worsened environment problems, great expectation has been focused on 3D carbon with excellent adsorption ability for environmental pollutants.[11]

As an isostructure of carbon, hexagonal boron nitride (hBN) has been called as "white graphite".[12-15] Porous boron nitride exhibits preeminent physical and chemical properties.[16-21] These characteristic make porous boron nitride a promising candidate.[22] Numerous researches has been done on BN to study its performance on removal of organic solvents[23] organic dyes[24] and metallic ions[25] from air or drinking water. It is noted that the studies on 3D boron nitride (3D BN) are developing very fast. Lian et al. presented a facile solid phase method for preparing unique 3D hBN nanoflowers, which showed good thermal stability and high specific surface area.[26] Liu et al. reported a 3D BN architectures consisted of an interconnected flexible network of nanosheets. This 3D BN architecture showed high specific surface area, excellent adsorption properties for organic dyes in aqueous solution as well as good reusability (88% of the starting adsorption capacity is maintained after 15 cycles).[27] In a very recent work, Zhao et al. developed a kind of 3D BN foam fabricated by a vesicant-assisted gas-foaming process. The product had a vesicular structure with hierarchical pores ranging from nm to μm scales and with ultrathin walls consisting of mono- or few-layered BN membranes with planar sizes as large as 100 μm. Their studies showed that the 3D BN foam exhibits superstrong adsorbent ability up to 190 times its own weight toward a wide range of environment contaminations, including several kind of oils and dyes.[28]

Herein, we report a method to synthesize a novel 3D nanostructure with hollow sphere shell morphology. The as-synthesized sample has high carbon content, which we named as 3D carbon boron nitride (3D C-BN). Our studies show that the prepared 3D C-BN sample displays excellent adsorption performance for dye (methylene blue, MB) in wastewater treatment, including high adsorption rates, large capacities and excellent reusability. More interestingly, the adsorption rate becomes higher when the 3D C-BN sample was used for the second time after desorption process. Our results indicate that the 3D C-BN can be regarded as promising adsorbent material for water cleaning.

2. Experimental

Material synthesis

The synthesis process of 3D C-BN is descripted as follows: Firstly, NH_4BF_4 and $NaBH_4$ with 1 : 1 molar rate were dissolved in right 1.4-diethylene dioxide at 40 ℃ under stirring, then got the filter liquor; Secondly, the mixed solvent was dried to obtain white gel (polymeric aminoborane, PAB)[29] at related high temperature. After that, same amount of melamine diborate (M2B), the preparation process has been described in another paper[24]) powder and the prepared white gel were

[a] Address here.School of Materials Science and Engineering, Hebei University of Technology, Tianjin 300130, P. R. China. E-mail:liuzhenya@hebut.edu.cn; tangcc@hebut.edu.cn; Fax : + 86-22-60202660; Tel : + 86-22-60202660.

dissolved in 1.4-diethylene dioxide solution under strongly stirring at 40 ℃, and then dried at 60 ℃ for 6 h. At last, the mixed white powder was heated to 1050 ℃ at a rate of 5 ℃ min^{-1} and kept for 4h in tube furnace. All reactions were carried out in a flow of N_2.

Characterization

The morphology of 3D C-BN was investigated by scanning electron microscopy (SEM, S-4800, HITACHI) and transmission electron microscopy (TEM, Tecnai F20, Philips).The structure of the sample was examined by X-ray powder diffraction analysis (XRD, D8 FOCUS, BRUKER). Fourier transformer infrared spectra (FTIR) were recorded on a Nicolet 7100 spectrophotometer between 400 and 4000 cm^{-1}. A double beam UV/vis spectrophotometer (U-3900H, HITACHI) was used to determine the concentration of dye in water samples. Conventional elemental analyzers (TC500 and CS230, Leco) were applied to analyse the detailed N, O, and C contents. X-ray photoelectron spectroscopy (XPS) was examined by a VGESCALAB 210 electron spectrometer. The nitrogen physisorption isotherms were measured at -196 ℃ on an AutoSorb iQ-C TCD analyzer. Prior to the measurement, the samples were activated in a vacuum at 300 ℃for 3 h. The Brunauer-Emmett-Teller (BET) specific surface area was calculated from the nitrogen adsorption data in the relative pressure ranging from 0.01 to 0.3.

3. Results and Discussion

Characterization

3D C-BN shows white, even the carbon content measured by conventional elemental analyzers reaches to 3.0 w% (Table 1). The measured composition for O is 18.7 w% and for N is 40.1 w%. Meanwhile, we also get the corresponding compound composition as B 0.373, C 0.039, N 0.398 and O 0.190 by XPS analysis. Figure 1(a) shows the SEM image of the 3D C-BN. The sample has a three dimensional morphology of many broken hollow spherical shells, which can be confirmed in the enlarged SEM image showed in Figure 1(b). An individual microsphere with a diameter of ~ 4 μm and a thickness of ~ 40 nm can be clearly observed. TEM image is given in figure 1(c), indicating the same result obtained by SEM. The inset picture is the SAED pattern taken from the edge of the broken hollow spherical shell reveals the hexagonal structured characteristic of the sample. Rings can be indexed to the (002), (100), (110) diffractions of hBN, respectively. The 3D C-BN's interspacing layers is ~ 0.35 nm. Figure 1(e) shows the XRD pattern of the white powder, in which all the diffraction peaks can be indexed to planes of hBN (Card No. 34-0421).[30] The peaks look highly broadened with a big Full Width at Half Maximum (FWHM). The pattern is handled by peak fitting and calculating with Scherrer Equation. The crystallinity is 62.6%, and the crystallite size is about 1.8 nm, which match well with the HRTEM imagine. FTIR spectrum of the 3D C- BN is shown in figure 1(f). The surface bonds indexed by the absorbance peaks are listed as follows, B-OH/B-NH_2 (~ 3421 and ~ 3257 cm^{-1}), C=O(~ 1630 cm^{-1}), B-N(~ 1400 cm^{-1}), B-N-O(~ 1160 cm^{-1}), C-O(~ 1080 cm^{-1}), B-N-O(~ 930 cm^{-1}), and BN-B(~ 800 cm^{-1}).[31,32]

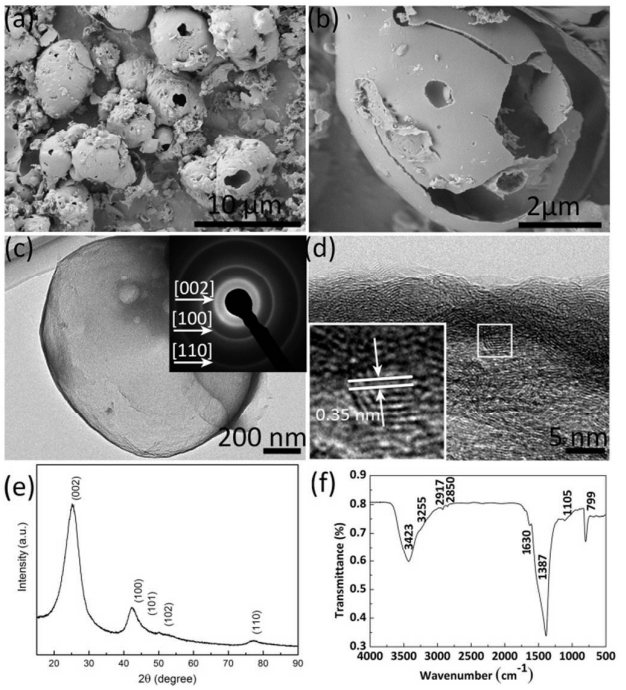

Fig. 1 (a) SEM image of 3D C-BN. (b) High magnification SEM image showing an individual hollow spherical shell. (c) Typical TEM images of the 3D C-BN. Inset is the corresponding SAED pattern. (d) HRTEM image of the shell. The layer distance is about 0.35 nm. (e) XRD pattern of 3D C-BN. (f) FTIR spectra of 3D C-BN.

Adsorption properties

Organic dyes are recognized as one of the main industrial pollution sources in the world can cause great harm to people's daily life and natural environment by polluting drinking water.[33] Wastewater treatment has become the focus of environmental protection. In order to study the adsorption properties of 3D C-BN, 100 mg 3D C-BN were added into 100 ml of MB solution with an initial concentration of 50 mg L^{-1}. The UV-Vis spectra data were collected at different time intervals, which are showed in Figure 2(a). Figure 3(b) gives the corresponding adsorption rate curve. After 90 min, the MB had been completely absorbed by 3D C-BN at room temperature. Corresponding photographic images of MB solution collected at different times after adding 3D C-BN were given in the inset of figure 2(c), showing the water becoming clean. The adsorption isotherm applied to Langmuir model[34] that well fits with experimental data with the correlation coefficient of 0.99 is showed in figure 2(e). Langmuir model is used to represent the relationship between the equilibrium solute concentration and the equilibrium adsorption capacity:

$$Q_e = Q_m K C_e/(1+KC_e) \qquad (1)$$

Where the Q_m is the maximum adsorption capacity corresponding to complete monolayer coverage (mg L^{-1}), K is the equilibrium

constant (L mg^{-1}), C_e is the equilibrium solute concentration (mg L^{-1}), and Q_e is the adsorbed amount of the dye at equilibrium concentration (mg L^{-1}).

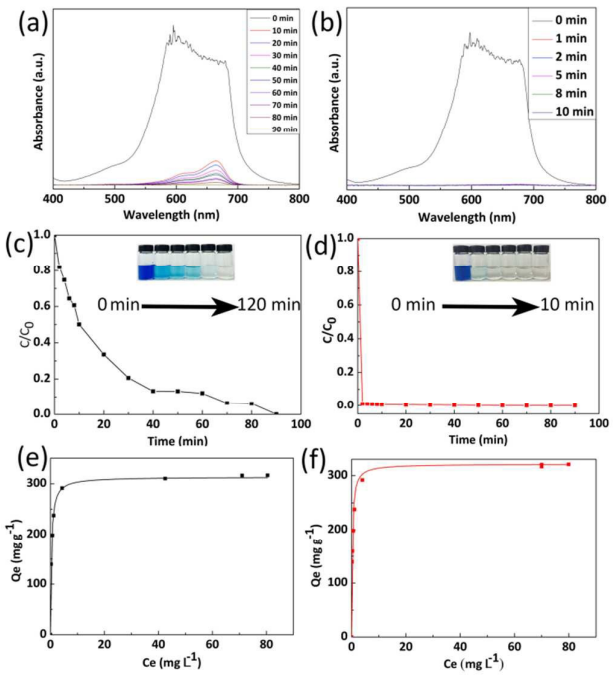

Fig. 2 adsorption performance of dyes (MB) on the 3D C-BN sample. (a) UV-vis absorption spectra of the aqueous MB solution (50mg L^{-1},100 mL) in the presence of 3D C-BN at different time intervals, respectively. (b) UV-vis absorption spectra of MB solution using the 1st-recycled 3D C-BN sample as adsorbent. (c) Corresponding adsorption rates of MB, insert is the visual variation of MB solution with time. (d) Corresponding adsorption rate and visual variation of MB solution on 1st-recycled 3D C-BN with time. (e) Adsorption isotherms of MB. (f) Adsorption isotherms of MB on the 1st-recycled 3D C-BN sample.

The maximum adsorption capacity of 3D C-BN for MB is 313.15 mg g^{-1}, higher than the BN nanocarpets,[35] fibre carbon,[36] and graphene[37] that have been reported before. The prominent adsorption capacity of 3D C-BN is responsible for the abundant surficial functional species,[26] such as –OH, resulted from our specially designed synthesis procedure. After adsorption, the 3D C-BN was recycles by heating up to 400 ℃ in the air for one hour.[38] Interestingly, we found that after the first regeneration cycle, the newly generated 3D C-BN named as 1st-recycled 3D C-BN displays highly enhanced adsorption performance. Figure 2(b) shows the recycled sample's UV-visible sorption spectra, indicating a dramatic change compared with Figure 2(b). The adsorption rate of the 1st-recycled 3D C-BN is obviously faster than the raw one. The MB is removed from the water less than two minutes (Figure 2(d)). Figure 2(f) shows the adsorption isotherm applied to Langmuir model. The maximum adsorption capacity Q_m of the 1st-recycled 3D C-BN is 321.43 mg g^{-1} and well fits with experimental data with the correlation coefficient $>$ 0.99. Figure 3 gives the cycle number of the 3D C-BN. The recycled materials could almost maintain the same adsorption capacity within 5 runs. After eight cycles, the capacity of C-BN remains more than 95%. Morphology of the raw sample and the 8th-recycled one were compared by the SEM image (Figure S2). The hollow spherical shells in raw sample have been broken into pieces after several times reused, and this is suggested to be the reason of the decreased capacity. Obviously, the high stability and reuse ability make the 3D C-BN extremely appropriate to be used as an efficient dyes adsorption material.

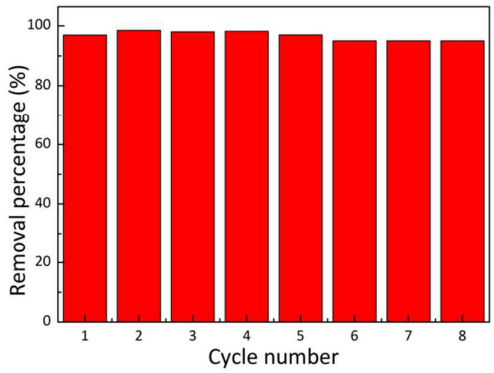

Fig. 3 Adsorption ability of MB on 3D C-BN in 8 successive cycles of desorption-adsorption (initial MB concentration: 50mg L^{-1}).

It seems so interesting that the adsorption rate of the 1st-recycled 3D C-BN sample is obviously higher than the raw one. The reason of the enhanced adsorption rate is attributed to the increased C content and the elimination of undesired esters molecules. Conventional elemental analyzers were applied to analyse the detailed N, O, and C contents of the raw sample, the 1st recycled one and the 2nd-recycled one (Table 1). It is clearly that the C content has been obviously increased after adsorption-desorption cycles, because of the incomplete combustion of MB. XRD pattern of the 1st recycled sample shows very little difference with the raw one in phases and crystallinity, so the increased C is suggested to be graphite and activated carbon, which would contribute to adsorption rate and capacity. Figure 4 shows the FTIR spectra of the raw sample and the 1st-recycled one. The peaks located on 2920 cm^{-1} and 2854 cm^{-1} in the raw 3D C-BN sample's spectra, corresponding to the C-H antisymmetric and symmetric stretching vibration, were almost disappeared in the 1st-recycled one. While the peak at 1630 cm^{-1} of C=O stretching and the double peaks at 1170 cm^{-1} and 1110 cm^{-1} of C-O-C stretching were also disappeared. It is suggested that there are some esters molecules attached on the raw 3D C-BN grains, which decrease the adsorption activity of the surficial functional species. This undesired esters molecules are eliminated after desorption process, which lead to a sharp raise of the adsorption rate. The HRTEM imagines (Figure 5) of these two samples coincide with this inference. We can see definite fringe corresponding to (002) plane in the image of 1st-recycled sample. In vivid contrast, only fuzzy fringes can be observed in the raw one, suggesting the existence of those undesired esters molecules.

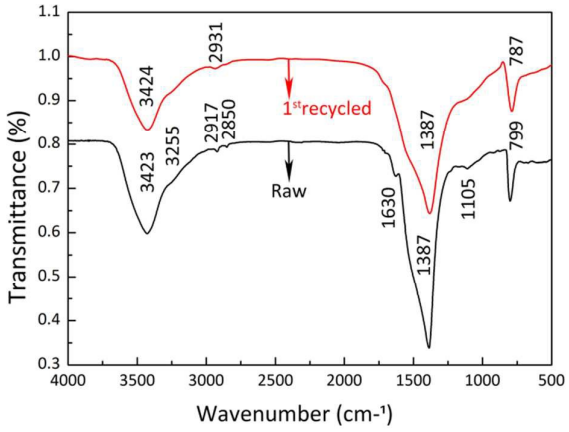

Fig. 4 comparison of FTIR spectra between the original sample and the 1st-recycled sample.

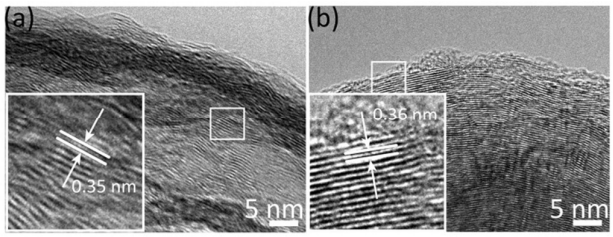

Fig. 5 (a) The corresponding HRTEM image of the original sample. (b) The corresponding HRTEM image of the recycled sample.

Sample	*C (w%)*	*N (w%)*	*O (w%)*
Raw	3.0	40.1	18.7
1st-recycled	9.2	35.9	18.9
2nd-recycled	9.9	32.8	24.3

Table 1. C, N and O concentration of the original 3D C-BN sample and recycled samples.

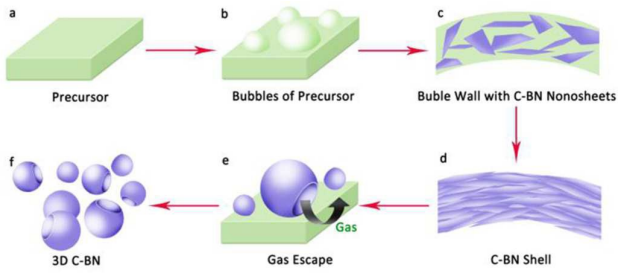

Fig. 6 Experimental scheme of the synthesis method of 3D C-BN.

Based on the above-mentioned experimental results and analysis, the synthesis method of 3D C-BN including high-temperature pyrolysis and self-bubbling is illustrated in figure 6. The precursor powders change gradually into a series of B – N – H polymeric forms such as polymeric aminoborane(PAB), $(H_2BNH_2)_n$, polyiminoborane(PIB), $(HBNH)_n$, and the BN matrix with a small quantity of hydrogen while the heat treatment started.[39] It is very easy for these B – N – H polymeric forms and M2B precursor to release H_2 or other gas, which can blow the precursor into bubbles (Figure 6(b)). Hexagonal carbon and BN nanosheets are generated in the bubble's wall during the high-temperature pyrolysis process, and then fabricate C-BN shells. Since the released gas accumulated, the C-BN bubbles are blasted from the inside and final become that broken hollow sphere shell like morphology(Figure 6(f)).[40] Additionally, the introduction of M2B into the precursor can increase the C content of 3D C-BN, which improve surface functional groups for the removal of MB.[41] The further investigation is on the way.

4. Conclusions

In summary, we have successfully synthesized a new kind of 3D C-BN nanomaterial with morphology of broken hollow spherical shells via a high-temperature pyrolysis and self-bubbling method. The 3D C-BN sample presents significant adsorption performance of organic dyes. The maximum adsorption capacity of MB on the 3D C-BN reaches to 313.15 mg g^{-1}, and the removal efficiency of 95% is maintained even after 8 times recycle. The adsorption rate becomes real high after one adsorption-desorption cycle. More importantly, MB can be totally removed in less than 2 minutes. Therefore, it will bring us lots of conveniences as well as it can save more resources in the practice.

5. Acknowledgements

This work was supported by the National Natural Science Foundation of China (Grants No. 51372066 and No.51172060), the Program for Changjiang Scholars and Innovative Research Team in University (PCSIRT: Grant No.IRT13060), the Innovation Fund for Excellent Graduate Student of Hebei Province (Grant No. 220056), the Natural Science Foundation of Hebei Province (Grant No. B2015202079).

1 B. Weng, S. Liu, Z. Tang and Y. Xu; RSC Adv., 2014, **4**, 12685-12700.
2 Y. Chen, C. Tan, H. Zhang and L. Wang; Chem. Soc. Rev., 2015, **44**, 2681-2701.
3 Z. Yu, H. Yuan, K. Lu, Y. Zhang and Z. Wei; RSC Adv., 2012, **2**, 338-343.
4 X. Xia, J. Tu, Y. Zhang, Y. Mai, X. Wang, C. Gu, and X. Zhao; J. Phys. Chem. C., 2011, **115**, 22662–22668.
5 H. Minamimoto, H. Irie, T. Uematsu, T. Tsuda, A. Imanishi, S. Seki, and S. Kuwabata; Langmuir, 2015, **31**, 4281−4289.
6 J. Lewis, J. Smay, J. Stuecker and J. Cesarano; J. Am. Ceram. Soc., 2006, **89** [12] 3599–3609 .
7 H. Ng, J. Li, M. Smith, PhoNguyen, A. Casse, J. Han, M. Meyyappan; Science., 2003, **300**, 1249.
8 International Technology Roadmap for Semiconductors 2001 (Semiconductor Industry Association, San Jose, CA,2001)

9 M. Serrano, M. Gutiérrez, F. Monte; Progress in Polymer Science., 2014, **39**, 1448–1471.
10 G. Gruner; Anal Bioanal Chem., 2006, **38**, 4: 322–335.
11 T. Wu, M. Chen, L. Zhang, X. Xu, Y. Liu, J. Yan, W. Wang and J. Gao; J. Mater. Chem. A., 2013,**1**, 7612-7621.
12 H. Zeng, C. Zhi, Z. Zhang, X. Wei, X. Wang, W. Guo, Yoshio Bando, and Dmitri Golberg; Nano Lett., 2010, **10**, 5049–5055.
13 J. Li, H. Luo, J. Lin, Y. Xue, Z. Liu, P. Jin, X. Xu, Y. Huang, D. Liu, J. Zhang and C. Tang; Materials Research Express., 2014, **1**, 035035.
14 W. Lei, Vadym N. Mochalin, D. Liu, S. Qin, Yury Gogotsi and Y. Chen; Nature Communications 2015, 6, 8849.
15 W.i Lei, D. Liu and Y. Chen; Adv. Mater. Interfaces 2015, 2, 1400529.
16 H. Wada; K. Nojima; K. Kuroda; C. Kato; Journal of the Ceramic Association Japan., 1987, **95**:130-134.
17 C. Zhi, Y. Bando, C. Tang, H. Kuwahara, and Golberg; Adv. Mater., 2009, **21**, 2889.
18 R. Gao, L. Yin, C. Wang, Y. Qi, N. Lun, L. Zhang, Y. Liu, L. Kang and X. Wang; J. Phys. Chem. C., 2009, **113**, 15160–15165.
19 J. Pattanayak, T. , Kar, and S. J.Scheiner; Ball. Phys. Chem. A., 2002, **106**, 2970–2978.
20 D. Liu, L. He, W. Lei, Karel D. Klika, L.Kong and Y.Chen; Adv. Mater. Interfaces 2015, 1500228.
21 D. Liu, W. Lei, S. Qin, Karel D. Klika and Y.Chen; Phys. Chem. Chem. Phys., 2016, 18, 84-88.
22 J. Li, J. Lin, X. Xu, X. Zhang, Y, J. Mi, Z. Mo, Y. Fan, L. Hu, X. Yang, J. Zhang, F. Meng, S. Yuan and C. Tang; Nanotechnology., 2013, **24** ,155603 (7pp).
23 G. Postole, A. Gervasini, C.e Guimon, A. Auroux and B. Bonnetot; J. Phys. Chem. B., 2006, **110**, 12572-12580.
24 J. Li, H. Jia, Y. Ding, H. Luo, Abbas Saleem, Z. Liu, L. Hu, C. Tang; Nanotechnology., 2015, Volume 26, Number 47.
25 W. Lei, David Portehault, D. Liu, S. Qin and Y. Chen; nature communications, 2013, **4**:1777.
26 J. Li, X. Xiao, X. Xu, J. Lin, Y. Huang, Y. Xue, P. Jin, J. Zou, C. Tang; SCIENTIFIC REPORTS, 2013, **3** : 3208.
27 G. Lian, X. Zhang, M. Tan, S. Zhang, D. Cui and Q.Wang; J. Mater. Chem., 2011, **21**, 9201.
28 D. Liu, W Lei, S. Qin and Y. Chen; physical chemistry two-dimensional materials., 2013, **4** : 4453.
29 H. Zhao, X. Song and H. Zeng; NPG Asia Materials., 2015, **7**, e168.
30 X. Wang, C. Zhi, L. Li; Advanced materials., 2011, **23**(35): 4072-4076.
31 C.Tang, Y. Bando,Y. Huang,C. Y. Zhi and D. Golberg; Adv. Funct.Mate, 2008, **18**, 3653–3661.
32 R. Nemanich, S. Solin and R. Martin; Phys. Rev. B., 1981, **23**, 6348.
33 C. Zhi, Y. Bando, C. Tang and D.Golberg; Appl. Phys. Lett., 2005, **86**, 213110.
34 E. Forgacs, T. Cserha ´ti and G. Oros; Environ. Int., 2004, **30**, 953–971.
35 X. Wang, Y. Zhong, T. Zhai, Y. Guo, S. Chen, Y. Ma, J. Yao, Y. Bando, D. Golberg; J. Mater. Chem., 2011, 21, 17680–17687.
36 X. Zhang, G. Lian, S. J. Zhang, D. L. Cui and Q. L. Wang; Cryst. Eng. Comm., 2012, 14, 4670–4676.
37 S. Senthilkumaar, P. Varadarajan, K. Porkodi, C. Subbhuraam; Journal of Colloid and Interface Science., 2005, 284 , 78–82.
38 T. Liu, Y. Li, Q. Du, J. Sun, Y. Jiao, G. Yang, Z. Wang, YXia, W. Zhang, K. Wang, H. Zhu, D. Wu; Colloids and Surfaces B: Biointerfaces., 2012, 90, 197–203.
39 J. Ll, Y. Huang, Z. Liu, J. Zhang, X. Liu, H. Luo, Y. M, X. Xu, Y. Lu, J. Lin, J. Zou and C.Tang; J. Maxter. Chem.A.,2015,3,8185.
40 X. Wang, A. Pakdel, C. Zhi, K. Watanabe, T.Sekiguchi, D. Golberg and Y. Bando; J. Phys.: Condens. Matter., 2012,24, 314205(9pp).
41 X. Zhang, Z. Lu, J. Lin, Y. Fan, L. Li, X. Xu, L. Hu, F. Meng, J. Zhao and C. Tang; ECS Journal of Solid State Science and Technology., 2013, 2 (3) R39-R43.

Three-dimensional carbon boron nitride with the broken hollow spherical shell for water treatment

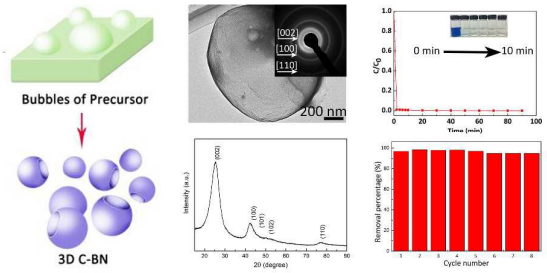

Broken hollow spherical shell like 3D C-BN with real fast adsorption rate of dyes for water purification